Imaging the Cardiovascular Pulse

Nanfei Sun
Dept. of Computer Sc.
Univ. of Houston
Houston, TX
nsun@mail.uh.edu

Marc Garbey
Dept. of Computer Sc.
Univ. of Houston
Houston, TX
garbey@cs.uh.edu

Arcangelo Merla
Dept. of Clinical Sc.
Univ. G. D'Annunzio
Chieti, Italy
a.merla@itab.unich.it

Ioannis Pavlidis
Dept. of Computer Sc.
Univ. of Houston
Houston, TX
ipavlidi@central.uh.edu

Abstract

We have developed a novel method to measure human cardiac pulse at a distance. It is based on the information contained in the thermal signal emitted from major superficial vessels. This signal is acquired through a highly sensitive thermal imaging system. Temperature on the vessel is modulated by pulsative blood flow. To compute the frequency of modulation (pulse), we extract a line-based region along the vessel. Then, we apply Fast Fourier Transform (FFT) to individual points along this line of interest to capitalize on the pulse propagation effect. Finally, we use an adaptive estimation function on the average FFT outcome to quantify the pulse. We have tested the accuracy of our method on 5 subjects with highly successful results. The technology is expected to find applications among others in sustained physiological monitoring of cardiopulmonary diseases, sport training, sleep studies, and psychophysiology (polygraph).

1. Introduction

Monitoring of cardiac pulse is widely used in health care, sport training, sleep studies, and psycho-physiological (polygraph) examinations. Various contact measurement methods have been developed to estimate a subject's cardiac pulse. The golden standard for pulse measurement is Electro-Cardio-Graphy (ECG) [1]. ECG records the differences of the electric potential generated in different regions of the body due to the propagation of the action potential in the cardiac muscular fibers. ECG recording requires the use of a signal amplifier and at least three electrodes.

When one is interested mainly in the cardiac frequency and not in the exact shape of the cardiac signal, simpler pulse measurement devices can be used. Such devices compute the pulse through indirect effects of blood flow change in the vascular network of a tissue.

The piezoelectric transducer is a classical cardiac pulse measurement device, which registers local changes in blood pressure associated to the cardiac activity as a voltage signal. It is instrumented with a probe that is typically attached to a finger of the subject [2]. This is a reliable method, but it is very sensitive to motion. The subject must stay still, because even slight finger motion will introduce substantial noise and cause signal fading. We use a piezoelectric device as the ground truth standard of comparison against our thermal imaging analysis method [3].

Doppler ultrasound is a more advanced technology, which has been used to collect blood velocity spectra. The full pulse waveform of the carotid has been recovered based on the blood velocity spectra by D.W. Holdsworth et al. in 1999 [4].

To the best of our knowledge, no contact-free pulse measurement method based on passive sensing has been demonstrated so far. Recently, Pavlidis et al. have proposed a series of bioheat and statistical models that in combination with customized highly sensitive thermal imaging hardware can measure various physiology variables from several feet away from the subjects. These include contact-free measurements of perfusion [5], vessel blood flow [6], and breathing rate [7].

In this paper, we describe an FFT based signal processing method to estimate in a contact-free manner the cardiac pulse of human subjects using thermal video sequences. We present a brief introduction to the pulse physiology in section 2. In section 3, we describe how to select and track the line-shaped region of interest on the tissue imagery. In section 4, we describe a novel method to apply FFT along this line-shaped region to capitalize upon the pulse propagation effect. In section 5, we describe the estimation function we apply on the average FFT result to extract the heartbeat frequency. In section 6

0-7695-2372-2/05/$20.00 (c) 2005 IEEE

we discuss the experimental setup and results. We conclude the paper in section 7.

2. Cardiovascular Pulse

The cardiovascular pulse is generated in the heart, when the chambers contract and blood bursts into the aorta from the left chamber. The blood travels through the arterial network and returns back to the heart through the vein network. Different mechanical processes are involved into the propagation of the cardiac pulse. Therefore, the pulse waveform can be described in terms of blood velocity, blood flow rate, and blood pressure. A comprehensive annotation to the pulse waveform was presented by D. W. Holdsworth in 1999 [4]. In that research, measurements were carried out on the carotid of the subjects by using Doppler ultrasound. Seven feature points correlated to the vascular fluid dynamics were identified as waveform descriptors (see Figure 1(a)). Comparing 3560 carotid waveforms from 17 subjects, the study reported negligible contralateral differences. This indicated that pulse waveforms of normal subjects have similar shapes.

In our study, we are interested in monitoring cardiovascular pulse through analysis of skin temperature modulation. Pulsative blood flow modulates tissue temperature because of the heat exchange by convection and conduction between vessels and surrounding tissue. Such modulation is more pronounced in the vicinity of major superficial blood vessels.

In [6] we have proposed a model to simulate the heat diffusion process on the skin initiated by the core tissue and a major superficial blood vessel. We also took into account noise effects due to the environment and instability in the blood flow. Our simulation demonstrated that the skin temperature waveform is directly analogous to the pulse waveform. But, its exact shape is smoothed, shifted, and noisy with respect to the originating pulse waveform due to the diffusion process and air flow. Figure 1(b) shows the skin temperature modulation computed by the 2D unsteady bioheat model in [6]. Comparing Figure 1(a) with Figure 1(b), we observe that some feature points, which provide fine detail, are missing, but the basic waveform shapes are still similar. This indicates that the pulse can be recovered from the skin temperature modulation recorded with a highly sensitivity thermal camera and processed through an appropriate signal analysis method.

3. Regions of Interest

As a consequence of the tissue thermal diffusion, modulation of skin temperature is strongest along the superficial blood vessels. This is also predicted by our bioheat transfer model reported in [6] and has been verified by our experiments. Based on clinical and anatomical knowledge [8][9], we extract the cardiac pulse either from the radial artero-venous complex, or the external carotid complex, or the frontal branch of the superficial temporal artero-venous complex (see Figure 2).

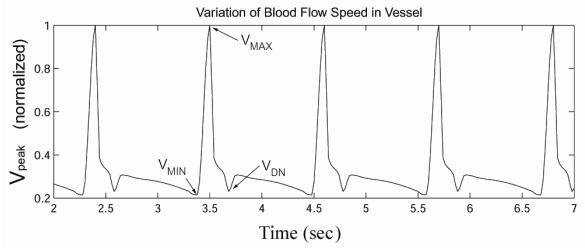

(a)

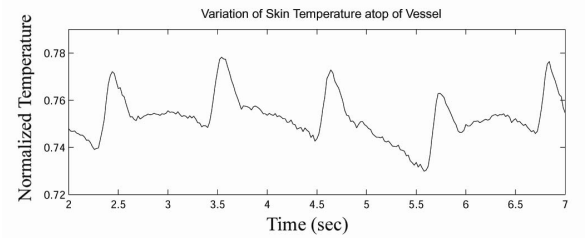

(b)

Figure 1: Pulse waveform given in: (a) Doppler ultrasound format [4]; (b) temperature modulation format produced by the 2D unsteady bioheat model [6].

Presently, we select the skin footprint of the vessel complex by manually drawing a line on the imagery through the graphical user interface. Therefore, the outcome depends on the skill and knowledge of the operator. In the future, vessel localization can be performed automatically by the computer, based on a superficial blood vessel segmentation method proposed by Pavlidis et al. [10]

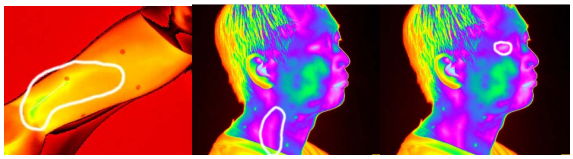

(a) (b) (c)

Figure 2: (a) Radial vessel complex. (b) Carotid vessel complex. (c) Superficial temporal vessel complex.

4. Pulse Measurement Methodology

Our method is based on the assumption that temperature modulation due to pulsating blood flow produces the strongest thermal signal on a superficial vessel. This signal is affected by physiological and environmental thermal phenomena. Therefore, the resulting thermal signal that is being sensed by the infrared camera is a composite signal, with the pulse being only one of its components. Our effort is directed into recovering the frequency of the component signal with the highest energy content. This is consistent with our hypothesis of pulse dominance in the thermal field of a superficial vessel.

As we mentioned in Section 3, we select interactively the pulse taking location in the first frame of the thermal video. A prerequisite to accurate pulse measurement is motion tracking. Even when subjects are instructed to stay put, they still exhibit slight movements due to motor functions. We use a conditional density propagation tracker [11] with thresholding as its feedback mechanism. The tracker allows meaningful application of Fourier analysis on the vessel's region of interest in the presence of tissue motion. Based on the outcome of Fourier analysis an estimation function computes the cardiac pulse. Figure 3 illustrates the general steps of our methodology.

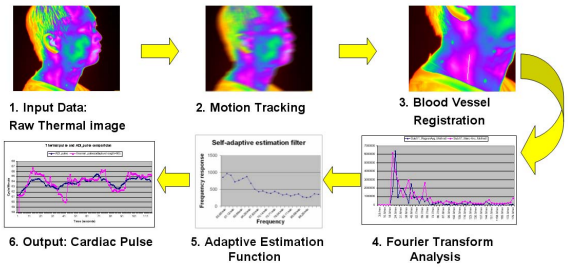

Figure 3: Pulse measurement methodology.

Considering that the blood vessel is a long, narrow structure, the pulse propagation phenomenon causes slight phase shift on the temperature profiles along the blood vessel. This may weaken the signal if we use conventional signal recovery methods in the time domain. Each pixel along the blood vessel has a unique periodical temperature profile, which is shifted with respect to the others. As Figure 4 shows, averaging these temperature profiles may weaken the signal. Although, the temperature profiles of the pixels along the blood vessel are shifted in the time domain, their frequency should remain the same

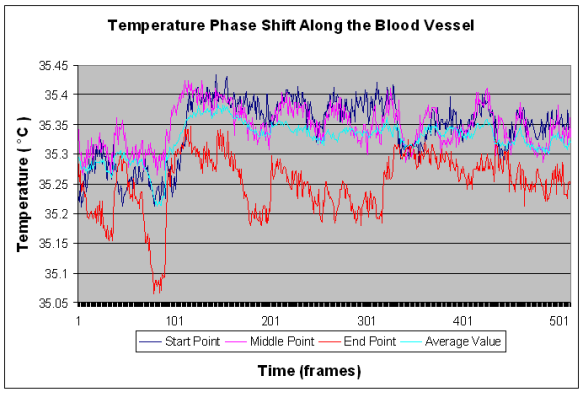

Figure 4: Temperature profiles of three different pixels along the exposed blood vessel compared to the average temperature profile.

(unshifted). Therefore, by operating on the frequency domain and combining appropriately the power spectra of these temperature profiles we can reinforce the signal instead of weakening it. We apply Fourier analysis in a novel manner to capitalize upon the pulse propagation effect and extract the dominant pulse frequency:

First Step: We select a straight segment L along the center line of a large superficial blood vessel. The algorithm expands symmetrically L into an elongated rectangle R. The width of this rectangle depends on the width of the vessel on the thermal imagery. For a subject imaged at 6 ft with a 50 mm lens the rectangle's width is 3-7 pixels. By convention, we place the x axis of our coordinate system along the width and the y axis along the length of the vessel (see Figure 5).

Second Step: We record the time evolution of the pixel matrix delineated by rectangle R for N frames (N = 256 or 512). Thus, we produce a 3D matrix $A(x,y,t)$, where $0 \le x \le R_x, 0 \le y \le R_y$ is the spatial extent of rectangle R and $0 \le t \le N-1$ is the timeline.

Third Step: We average the pixel temperatures along the x dimension. Thus, we derive a 2D matrix:

$$A'(y,t) = \frac{1}{R_x}\sum_{x=0}^{R_x} A(x,y,t), \qquad (1)$$

where $0 \le y \le R_y, 0 \le t \le N-1$. This reduces the noise and "shrinks" the rectangular vessel region R into an *effective* line, upon which the signal measurement will be performed.

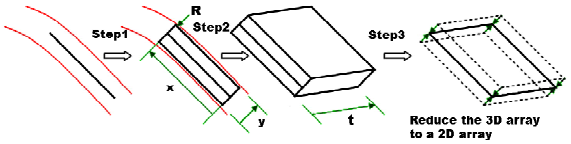

Figure 5: Schematic diagram of the first three steps in our Fourier analysis of the vessel temperature signal.

Fourth Step: For each *effective* pixel on the measurement line we obtain the time evolution signal of its temperature:

$$\{\forall y : S_y(t) = A'(y,t), 0 \le t \le N-1\}. \quad (2)$$

We apply the Fast Fourier Transform (FFT) on each of these signals to obtain the respective power spectra:

$$\{\forall y : \mathrm{P}_y = \mathscr{F}(S_y(t))\} \quad (3)$$

The FFT method was first introduced by Cooley and Tukey (1965) [12]. Thereafter, it was used widely in signal analysis due to its high efficiency in comparison to other methods, such as the solution of linear equations or the correlation method [13]. We apply a classical decimation-in-time (Cooley and Tukey) 1D base-2 FFT method given in [14].

Fifth Step: We average all the power spectra computed in the previous step into a composite power spectrum:

$$\bar{\mathrm{P}} = \frac{1}{R_y}\sum_{y=0}^{R_y}\mathrm{P}_y. \quad (4).$$

5. Adaptive Estimation Function

A fundamental question is what we report as the effective pulse along the timeline. The instantaneous computation described in Section 4 is not to be trusted literally since it may be affected occasionally by thermoregulatory vasodilation [15] and creeping noise. To address this problem we use an estimation function that takes into account the current measurement as well as a series of past measurements.

The current power spectrum $\bar{\mathrm{P}}_0$ of the temperature signal is being computed over the previous N frames (N = 256 or 512) by applying the process outlined in Section 4. We convolve the current power spectrum with a weighted average of the power spectra computed during the previous M time steps. We chose M=60, since at the average speed of 30 fps sustained by our system, there is at least one full pulse cycle contained within 60 frames even in extreme physiological scenarios. Therefore, the historical contribution to our estimation function remains meaningful at all times.

Specifically, the historical frequency response at a particular frequency f is given as the summation of all the corresponding frequency responses for the M spectra, normalized over the total sum of all the frequency responses for all the historical M spectra:

$$H(f) = \sum_{i=1}^{M}\bar{P}_i(f) / \sum_{i=1}^{M}\sum_{j=1}^{F}\bar{P}_i(j). \quad (5)$$

Finally, we convolve the historical power spectrum $\bar{H}$ with the current power spectrum to filter out transient features. We then designate as pulse the frequency f_{pulse} that corresponds to the highest energy value of the filtered spectrum within the operational frequency band.

6. Experimental Results

We have used a high quality Thermal Imaging (TI) system for data collection [16]. We have recorded 25 thermal clips from 5 subjects while resting in an armchair. Concomitantly we have recorded ground-truth pulse signals with PowerLab/4SP from AD Instruments featuring an MLT 1010 piezoelectric pulse transducer [17]. The sample has subjects of both genders, different ages, and with varying physical characteristics. In the case of wrist we have taken measurements before, during, and after the application of a forearm cuff. We have found no significant differences in the accuracy of the thermal imaging measurements among these scenarios.

Because our thermal imaging system and the PowerLab/4SP data acquisition system have different frequency of sampling and perform measurements on a vastly different theoretical basis, we need first to normalize the experimental data from the two modalities in order to compare them.

The PowerLab/4SP data acquisition system (ground truth) collects 100 samples per second, while our thermal imaging system acquires 30 frames per second. We average the ground truth output data every ten samples while the infrared thermal imaging data every three samples (frames). Based on this normalization, we have compared the average cardiovascular pulse rate computed by our imaging method to that reported by the ground-truth instrument for all the subjects in our data set.

TABLE I shows the detailed profile of our comparative experiment and the average pulse measurements reported by the two modalities. The

TABLE I

COMPARISON OF GROUND TRUTH AND THERMAL IMAGING PULSE MEASUREMENTS

Subject Number	Video File	Time Length (sec)	Tissue	Status of Pressure on Forearm	Ground Truth Pulse in bpm (X)	Thermal Imaging Pulse in bpm (y)	% Accuracy
Subject 01	D005-001	132.3	Neck	N/A	63.7	63.1	98.28
Subject 01	D005-002	121.4	Neck	N/A	60.3	60.8	99.22
Subject 01	D005-003	123.3	Wrist	No Pressure	62.1	62.9	98.68
Subject 01	D005-011	120.7	Wrist	No Pressure	67.9	68.0	99.88
Subject 01	D005-012	210.4	Wrist	Pressure	61.3	61.7	99.43
Subject 01	D005-013	240.5	Wrist	After Pressure	62.7	62.9	99.66
Subject 02	D005-016	120.7	Neck	N/A	82.7	80.5	98.01
Subject 02	D005-017	120.7	Neck	N/A	73.3	73.8	99.37
Subject 02	D005-018	120.6	Wrist	No Pressure	75.7	75.7	99.92
Subject 02	D005-019	180.7	Wrist	Pressure	74.8	74.6	99.76
Subject 02	D005-020	180.6	Wrist	After Pressure	78.5	78.2	99.72
Subject 03	D005-040	120.2	Neck	N/A	68.0	68.6	99.11
Subject 03	D005-041	122.5	Neck	N/A	65.6	66.5	98.68
Subject 03	D005-042	120.7	Wrist	No Pressure	63.8	64.3	99.32
Subject 03	D005-044	123.7	Wrist	After Pressure	68.2	68.3	99.34
Subject 03	D005-046	122.1	Forehead	N/A	67.4	67.8	99.34
Subject 04	D005-060	125.1	Neck	N/A	67.3	67.2	99.76
Subject 04	D005-062	121.0	Wrist	No Pressure	65.2	64.4	98.72
Subject 04	D005-063	180.8	Wrist	Pressure	63.7	64.7	98.54
Subject 04	D005-064	181.3	Wrist	After Pressure	72.1	71.1	98.66
Subject 04	D005-066	183.4	Forehead	N/A	66.8	67.3	99.27
Subject 05	D005-079	120.9	Neck	N/A	76.2	76.1	99.83
Subject 05	D005-080	117.1	Neck	N/A	72.6	71.9	99.03
Subject 05	D005-081	120.8	Wrist	No Pressure	70.7	71.7	98.67
Subject 05	D005-085	188.6	Wrist	After Pressure	73.2	73.5	99.59

overall agreement between the two measurement methods is 98%.

To quantify the linear correlation between the two measurement modalities, we have used the high Pearson product moment measure P_c [18]. By applying the Pearson formula on the data of TABLE I, we find that $P_c = 0.994$, which indicates a strong degree of correlation.

7. Conclusion

We presented a novel measurement method of cardiovascular pulse. The method is based on thermal imaging and exploits the quasi-periodic properties of the cardiac pulse through Fourier signal analysis. An adaptive estimation function ensures robust selection of the pulse frequency in the presence of signal noise. Since the method is contact-free, passive, and highly automated (imaging tracker), it opens the way for sustained physiological measurements in the most transparent manner.

Almost all the conventional methods require contact and hence they compromise the subject's comfort and mobility, especially in long observational periods. Moreover, measurements by these methods are strongly affected by movement artifacts with no easy way to counteract them.

Initially, our method may find applications in sleep studies, sport training, and psycho-physiological evaluations (polygraphy). In all these cases long observations are required and intrusive sensing is undesirable since it interferes with the subject's function. Therefore, a contact-free highly automated pulse measurement method will bring considerable value.

Our method exhibits a strong degree of linear correlation to a standard piezoelectric pulse measurement method we compared against. Although, the sample size is small and how well the method will scale up in a large data set is an open question, the feasibility of the approach has been clearly demonstrated.

8. Acknowledgements

We would like to thank the National Science Foundation (grant # IIS-0414754) and Dr. Ephraim Glinert, for their support and encouragement during the lifetime of this burgeoning research project.

Equally, we would like to thank the Computer Science Department of the University of Houston for providing additional support. The views expressed by the authors in this paper do not necessarily reflect the views of the funding agencies.

9. References

[1] A.C. Guyton, *Textbook of Medical Physiology*, 8th ed. Philadelphia, PA: W.B. Saunders Company, 1991, chapter 11.

[2] K. Aminian, X. Thouvenin, Ph. Robert, J. Seydoux, and L. Girardier, "A Piezoelectric Belt for Cardiac Pulse and Respiration Measurements on Small Mammals," *Proc.14th Ann. Inter. Conf. IEEE Eng. Med. Biol.*, 1992, pp. 2663-2664.

[3] *PowerLab ADInstruments Owner's Manual*, ADInstruments Pty Ltd, Unit 6, 4 Gladstone Rd, Castle Hill, NSW 2154, Australia, Document Number:U-PL/QS-002A, pp. 92.

[4] D. W. Holdsworth, C.J. Norley, R. Frayne, D.A. Steinman, and B.K. Rutt, "Characterization of common carotid artery blood-flow waveforms in normal human subjects," *Physiol. Meas.*, vol. 20, August 1999, pp. 219-240.

[5] I. Pavlidis and J. Levine, "Monitoring of periorbital blood flow rate through thermal image analysis and its application to polygraph testing," in *Proceeding of the 23rd Annual International Conference of the IEEE Engineering in Medicine and Biology*, Istanbul, Turkey, October 25-28, 2001.

[6] M. Garbey, A. Merla, and I. Pavlidis, "Estimation of blood flow speed and vessel location from thermal video," in *Proceedings of the 2004 IEEE Computer Society Conference on Computer Vision and Pattern Recognition*, vol. 1, Washington D.C., June 27-July 2, 2004, pp. 356-363.

[7] R. Murthy, I. Pavlidis, and P. Tsiamyrtzis, "Touchless monitoring of breathing function," in *Proceedings of the 26th Annual International Conference of the IEEE Engineering in Medicine and Biology*, San Francisco, California, September 1-5, 2004.

[8] R.R. Seeley, T.D. Stephens, and P. Tate, *Anatomy & Physiology*, 6th ed. New York: McGraw-Hill, 2003, pp.746.

[9] F.H. Martini, *Fundamentals of Anatomy & Physiology*, 6th ed. San Francisco, CA: Benjamin Cummings, 2004, pp.753.

[10] I. Pavlidis, P. Tsiamyrtzis, C. Manohar, and P. Buddharaju, "Biometrics: face recognition in thermal infrared," in *Biomedical Engineering Handbook*, N. Diakides, Ed. CRC Press, to appear in June 2005.

[11] M. Isard and A. Blake, "Condensation – conditional density propagation for visual tracking," *Int. J. Computer Vision*, vol. 19, no. 1, 1998, pp. 5-28.

[12] J.W. Cooley and J.W. Tukey, "An algorithm for the machine calculation of complex Fourier Series," Mathematics Computation, Vol. 19, 1965, pp 297-301.

[13] S.W. Smith. The Scientist and Engineer's Guide to Digital Signal Processing, San Diego, 2nd ed. CA: California Technical Publishing, 1999, pp. 225-242.

[14] William H. Press, Saul A. Teukolsky, William T. Vetterling, Brian P. Flannery. Numerical Recipes in C, 2nd ed. New York, New York: Cambridge University Press, 1992, pp. 504-521.

[15] N. Charkoudian, "Skin Blood Flow in Adult Human Thermoregulation," *Mayo Clin. Proc.*, vol. 78, May 2003, pp. 603-612.

[16] Indigo Systems, 70 Castilian Dr., Goleta, California 93117-3027, http://www.indigosystems.com.

[17] ADInstruments, 2205 Executive Circle, Colorado Springs, Colorado 80906, http://www.adinstruemnts.com.

[18] Karl Pearson, Mathematical Contributions to the Theory of Evolution. III. Regression, Heredity and Panmixia, Philosophical Transactions of the Royal Society of London. Series A, Vol.187, 1896, pp.253-318.